IOP Conf. Series: Materials Science and Engineering **252** (2017) 012040 doi:10.1088/1757-899X/252/1/012040

DESIGN AND ANALYSIS OF A FUSED DEPOSITION MODELLING MANUFACTURED PART

Claudiu DIACONESCU[1], Stefan TABACU[2], Alexandru OLTEAN[3]

[1]ALSECA Engineering, Bucharest, Romania; [2]University of Pitesti, Pitesti, Argeş, Romania

claudiu.diaconescu@alseca.com

Abstract. Fused deposition modelling (FDM) technology was investigated in order to produce a part designed to support a test load without permanent deformation. A topology optimization script was developed in order to define the final shape of the part. The solver used for the numerical analysis is LS-Dyna (implicit formulation). The algorithm follows the element removal based on the stress state and it can be very simply implemented. This solution of developing a custom code was adopted because plastic strain state was monitored and this is not yet implemented in other topology optimization applications. The results of the traction test were assembled and investigated in order to outline some of the typical parameters used for mechanical characterization. As a general overview of the results it was found that the parts manufactured using a 45°/45° stacking configuration are stronger that the ones manufactured using 0°/90° stacking configuration.

1. Introduction

Rapid prototyping consists in technologies capable to manufacture complex part in a short period of time. Without considering the costs related to infrastructure the parts are less expensive compared to the ones manufactured using conventional technologies. Another important aspect is that parts with internal voids can be manufacture.

Among the 3D printing technologies plays an important role [1] and plays an important role. Fused deposition modelling (FDM) [2] is one technique of rapid prototyping based of 3D printing that uses an extruded plastic wire in order to form complex part. The materials used to form the parts are similar to some currently used in injection molding technology [3].

Ahn et al. [4] investigated ABS P400 material as used for injection moulded parts and for parts manufactured using Fused Deposition Modelling. The influence of the raster orientation and the gap between two adjacent paths were identified as the major parameters that influence the mechanical performances of the parts manufactured using Rapid Prototyping techniques. A set of rules are outlined to conclude their work and provides a valuable start point in designing parts to be manufactures using FDM.

Also the work of Dawoud et al. [5] is focused on study of the mechanical behaviour of ABS. The raster angle and the gap are also in this case the main parameters associated with the manufactures parts. The printing process parameters were not altered from one part to other. It was found that using a negative gap can increase both traction and flexural performances of the part (up to -12% in performance compared to injection moulded specimens). The differences are explained also by the

structure of the material - injection moulding allows the formation of crystals while FDM results in an amorphous (yet less strong) structure.

Garg and Bhattacharya propose in their work [6] a numerical model that in capable to accurately describe by the mean of finite elements method the behave of structures under tensile loading. The method is applied to investigate specific specimens for tensile test. Results show a good agreement between the experiment and simulation results. The study completes the knowledge in the field showing that the strongest parts are obtained when the part is aligned with the building plane.

A study on the build parameters in case of fused deposition modelling developed by Griffiths et al. [7] points that the infill level and number of shells plays an important role when the improvement of mechanical properties of parts is addressed.

2. Investigation of the mechanical properties

In order to investigate the mechanical properties of ABS a number of samples were manufactured using MakerBoot Experimental 2X printer that used Fused Deposition Modelling technology for rapid prototyping. The specimens were tested in traction using a universal testing machine. The tests were performed according to the prescriptions of ASTM D 638.

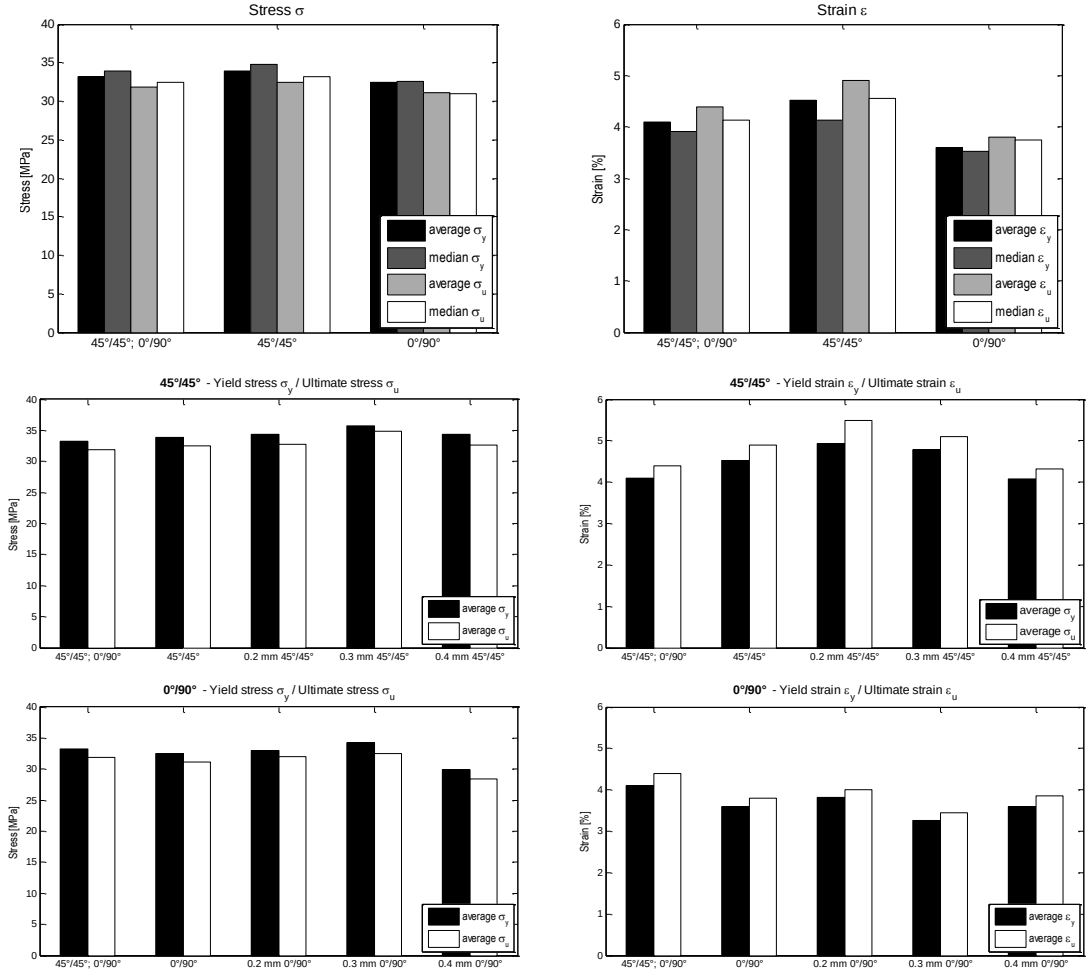

a) *b)*

Figure 1. Analysis results of the tensile tests.

a) overall results – stress yield/ultimate; b) overall results – strain yield / ultimate;

The results of the traction test were assembled and investigated in order to outline some of the typical parameters used for mechanical characterization. As a general overview of the results it was found, as expected and also supported by literature [5], that the parts manufactured using a 45°/45° stacking configuration are stronger [8] that the ones manufactured using 0°/90° stacking configuration (Figure 1 *a)*).

In case of a 45°/45° configuration, Figure 1 *c)* show that increasing the layer thickness the strength of the part increases. However the increase of the layer thickness results in a decrease of the strain as resulting from Figure 1 *d)*. A smaller layer thickness gives a more compact construction yet the raw material might be affected during extruding thus the mechanical properties altered. This gives the small decrease in strength. The higher value of the stress is recorded for a layer thickness of .3 mm close to the optimal value recommended for the 3D printer.

For the 0°/90° there is a similar pattern. The stress increases with the increase of the layer thickness (Figure 1 *e)*) while the strain decreases (Figure 1 *f)*)

The fractured sections of the parts are presented in Figure 2. Figure 2 *a)* presents the cross section of the 45°/45° sample with a layer thickness of 0.2. The section shows some small voids on the edge (contour section). The voids [9] can also be explained by the standard configuration with a null gap. Figure 2 *b)* presents the cross section of the 0°/90° sample with a layer thickness of 0.4. The previous observations are also valid.

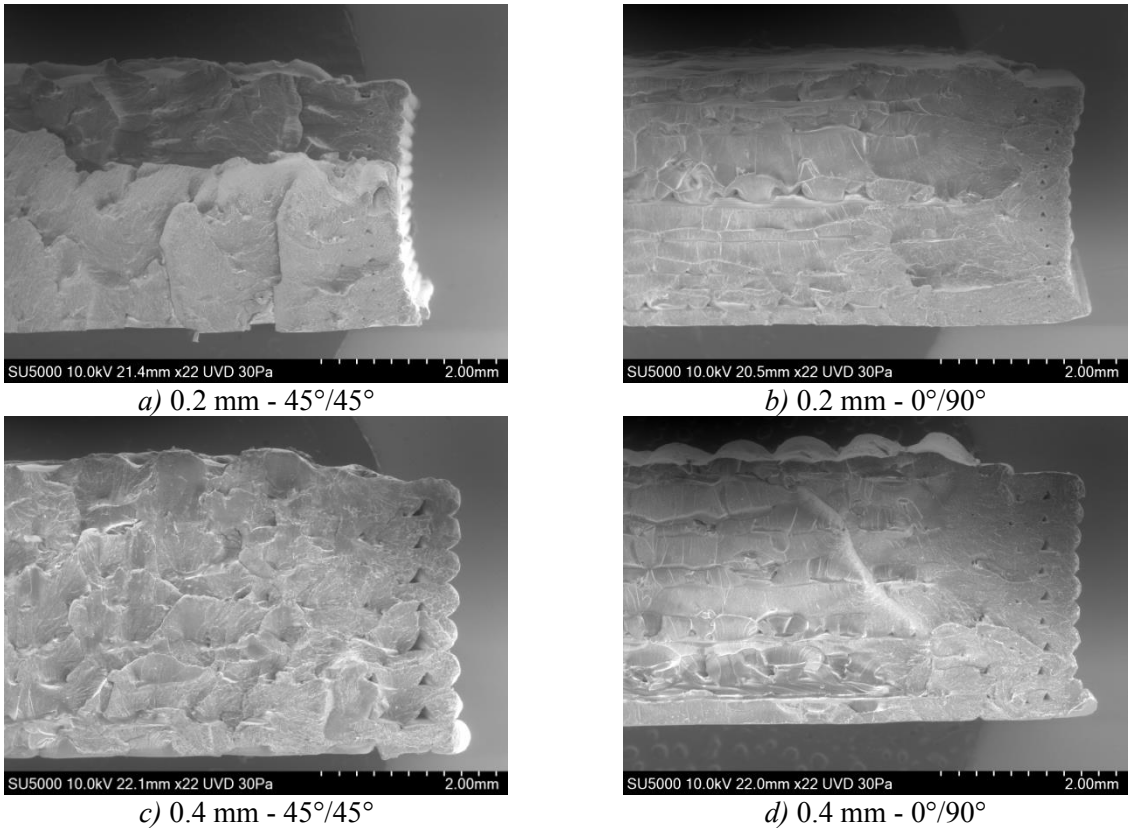

a) 0.2 mm - 45°/45° *b)* 0.2 mm - 0°/90°

c) 0.4 mm - 45°/45° *d)* 0.4 mm - 0°/90°

Figure 2. SEM images of the fractured section.

In the case of 45°/45° parts there is a similar pattern for the fractured section as presented in Figure 2 *a)*, *c)*. It worth mentioning that there is predominant direction for the failure of the material. However the part with a layer thickness of 0.4 mm displays more voids. The stress is lower because the number of longitudinal filaments.

Figure 3 *a)* displays the fracture pattern for a part with 0.3 mm layer thickness and a stacking sequence of 45°/-45°. It shows that the 45° and -45° filaments fused together. Figure 3 *a)* displays the fracture pattern for a part with a stacking sequence of 0°/-90°. The layers fused together. The failure is produced staring from the transverse filament followed by the failure of the longitudinal one.

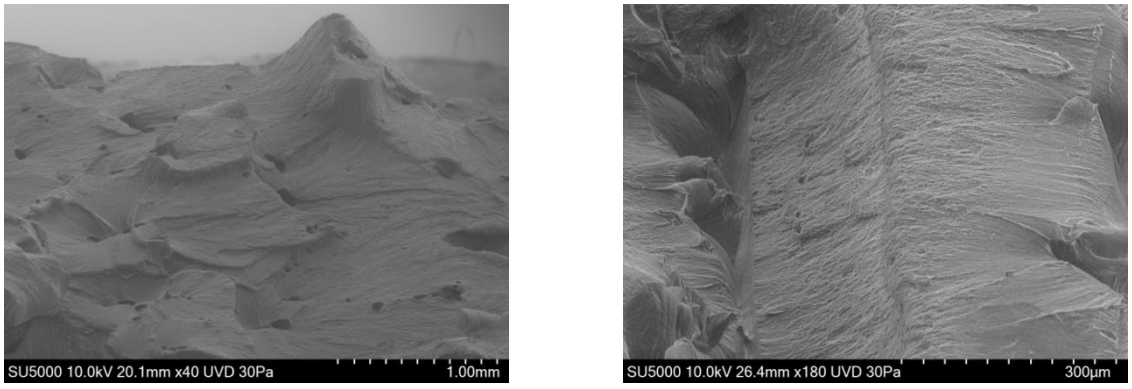

a) 0.3 mm - 45°/-45° *b)* 0.3 mm - 0°/90°

Figure 3. SEM images of the fractured section (details for the 0.3 mm layer thickness).

In order to provide an input for the design of part, Figure 4 presents typical stress – strain curves for the ABS material. Data presented follow the results of the analysis presented in Figure 1.

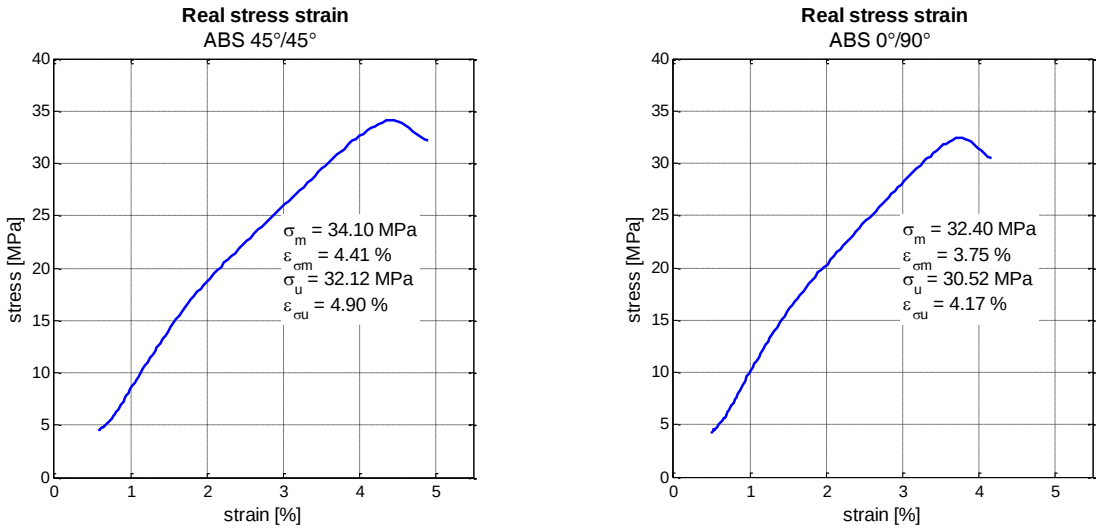

45°/-45° stacking sequence 0°/90° stacking sequence

Figure 4. Stress strain data for ABS.

Although literature displays for ABS values of the Young Modulus of 1950-2000 MPa the present study reports values between 1000-1100 MPa. For design purposes of the parts a value of 1050 MPa was recommended. Poisson's coefficient must be considered according to literature thus a value of 0.36 can be used.

3. Part design

A sample part is designed in order to support a load of 1500 N without permanent deformation. The part is considered to be clamped at the bottom supports and the load is applied at mid-span.

A topology optimization [10–12] script was developed in order to define the final shape of the part. The solver used for the numerical analysis [6] is LS-Dyna (implicit formulation). The algorithm follows the element removal based on the stress state and it can be very simply implemented. This solution of developing a custom code was adopted because plastic strain state was monitored and this is not yet implemented in other topology optimization applications.

The input data are obtained from the AVS database by *DATABASE_AVSFLT card in an ASCII format. The values reported are stress tensor components and the plastic strain.

For each step a stress value is imposed thus the elements with an associated value below that minimum are removed from the model. The function giving the threshold value can be adapted to different situations by the selection of the exponent parameter $stpexp$. The exponent should be selected according to each application as a function of the model size, load configuration, load magnitude and support configuration. For the current model a "conservative" exponent was selected (5.0). Additional parameters like nodal or rigid displacement can be imposed as termination criteria.

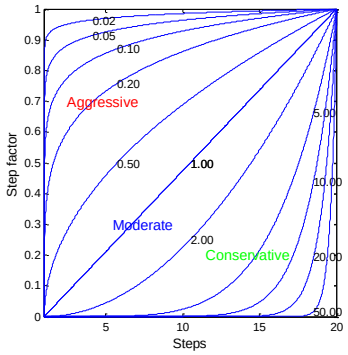

$$\sigma_c = \sigma_m \cdot \left(\frac{step}{steps}\right)^{stpexp}$$

User parameters:
σ_m - maximum stress state
$steps$ - number of steps for the optimization process
$stpexp$ - gives the current factor $\left(\frac{step}{steps}\right)^{stpexp}$

Figure 5. Optimization parameters.

The initial design domain (displayed in yellow) is presented in Figure 6 (step 1). It can be noticed that given the value of the $stpexp$ for the first steps the shape of the part doesn't change too much. The final steps defined the actual shape of the part. Considering 20 iterations the plastic strain limit was reached at iteration 15 thus the final shape of the part is the one obtained for step 14.

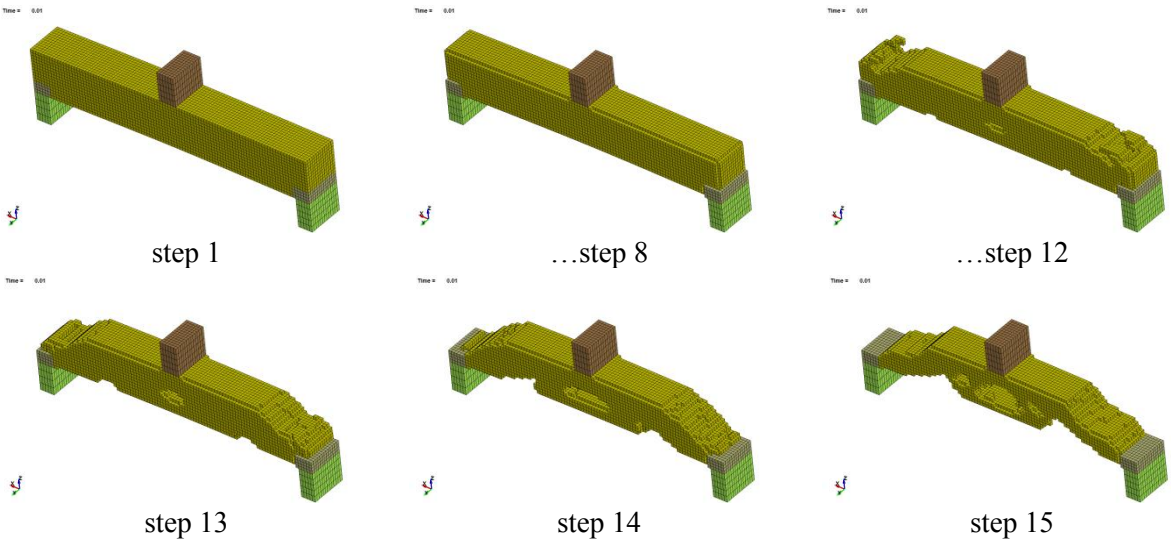

Figure 6. Optimization solution.

It should be mentioned that the section displayed in green and brown are add-on features intended to fix the part and to load it.

Considering the geometrical solution obtained after the optimization the part was printed using MakerBoot Experimental 2X printer. Figure 7 presents the outline of the part that it was designed following the optimization solution. Details on the printing pattern are provided for the narrow sections of the model.

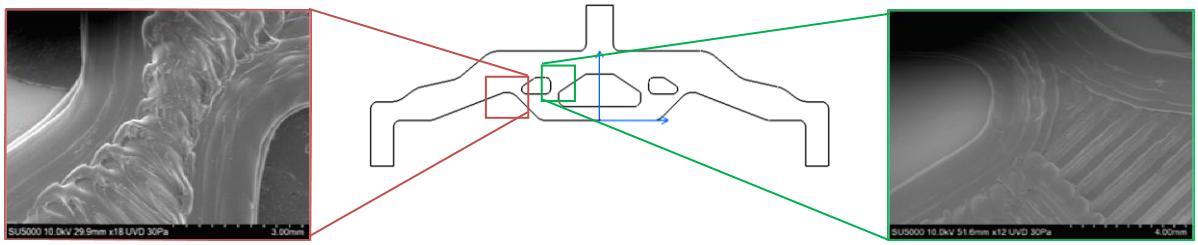

Figure 7. Outline of the part and details on the printing pattern.

4. Experimental investigation

The finished part was fitted on the universal testing machine using a custom 3 points bending fixture. The bottom left and right end were clamped while the load was applied on top of the part. The loading configuration if presented in Figure 8*a)*.

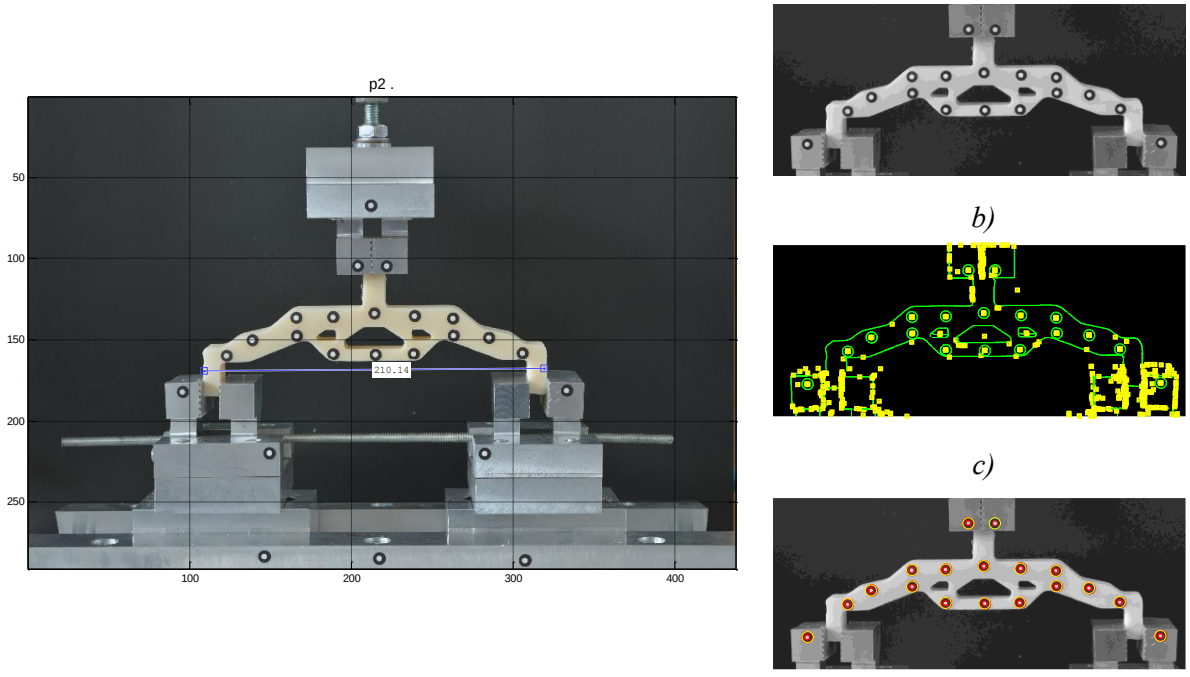

Figure 8. Experimental analysis of the part.

a) loading configuration; *c)-d)* image processing procedure.

The top displacement was recorded using the machine equipment. In order to improve the reading of the results and to obtain results for a complex deformation analysis a number of high resolution markers were added on the part.

Using digital camera, images of the part during loading were captured. Figure 8*b)* presents the first step of the video analysis. The colour image was processed to grey. Using edge-detection the positions of the markers were identified as presented in Figure 8*c)*. Considering the circular shape the centre of each marker was identified (Figure 8*d)*) and the coordinates were saved to a data file.

The markers located at the bottom of the machine were used as a reference in order to eliminate the motion of the camera during shooting. Considering the first recorded frame fixed the subsequent positions of the markers located on the machine were corrected. This was the actual deformed shape of the part can be determined.

Figure 9 present the positions of the markers during loading process. The initial state, final state and intermediary positions can be identified. This way there is a good traceability of each point and the global deformation can be correlated with local values.

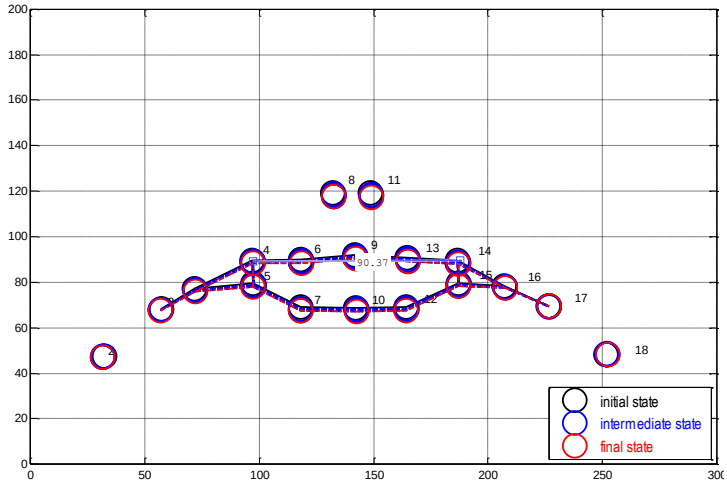

Figure 9. Deformation history of the part.

Figure 10 presents a comparison of the results as obtained from simulation and experiment. Overall there is a good agreement between the two sets of results. The nonlinear behaviour of the part as obtained from the experiment can be explained by the existence of friction between the mechanical parts.

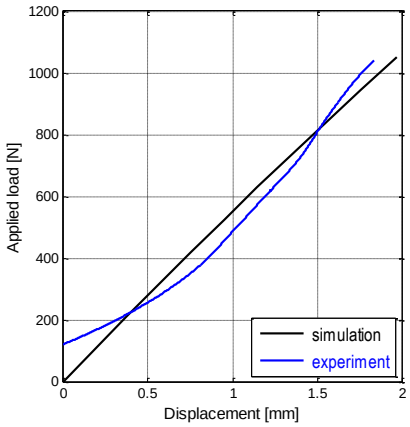

Figure 10. Displacement of the part at loading point.

The part is just a little bit stiffer than it was estimated by the model. This is considered acceptable as the numerical models should be considered conservative in order not to overestimate of to overcome some characteristics of the real model.

5. Conclusions

The present paper gives a brief description over the design and analysis process of a fused deposition modelling manufactured part.

The process debuted with the examination of the mechanical properties of the material. A number of specimens were manufactured and tested using a universal testing machine. Considering the number of parameters that can be controlled, the influences of stacking and layer thickness over the mechanical properties were investigated.

Once a global mechanical model was defined a part was constructed. The construction of the part is the results of an optimization process using numerical simulation by the finite elements method.

The part was finished using computer aided design and finally manufactured with a 3D printer.

In order to evaluate the performances a three-point bending experiment was developed. Image analysis was employed in order to enhance the results from the experimental analysis.

A good agreement was obtained between results from the numerical analysis and simulation. The small differences (showing a stiffer printed model) can be explained by the use of filleting radii that enhances flow stress. Nonlinearities can be explained by the existence of friction of the mechanical components of the testing equipment.

References

[1] Schniederjans D G 2017 Adoption of 3D-printing technologies in manufacturing: A survey analysis *Int. J. Prod. Econ.* **183** 287–98

[2] Thompson M K, Moroni G, Vaneker T, Fadel G, Campbell R I, Gibson I, Bernard A, Schulz J, Graf P, Ahuja B and Martina F 2016 Design for Additive Manufacturing: Trends, opportunities, considerations, and constraints *CIRP Ann. - Manuf. Technol.* **65** 737–60

[3] Carneiro O S, Silva A F and Gomes R 2015 Fused deposition modeling with polypropylene *Mater. Des.* **83** 768–76

[4] Ahn S, Montero M, Odell D, Roundy S and Wright P K 2002 Anisotropic material properties of fused deposition modeling ABS *Rapid Prototyp. J.* **8** 248–57

[5] Dawoud M, Taha I and Ebeid S J 2016 Mechanical behaviour of ABS: An experimental study using FDM and injection moulding techniques *J. Manuf. Process.* **21** 39–45

[6] Garg A and Bhattacharya A 2016 An Insight to the Failure of FDM Parts under Tensile Loading: Finite Element Analysis and Experimental Study *Int. J. Mech. Sci.*

[7] Griffiths C A, Howarth J, Rowbotham G D A and Rees A 2016 Effect of Build Parameters on Processing Efficiency and Material Performance in Fused Deposition Modelling *Procedia CIRP* **49** 28–32

[8] Zaldivar R J J, Witkin D B B, McLouth T, Patel D N N, Schmitt K and Nokes J P P 2017 Influence of processing and orientation print effects on the mechanical and thermal behavior of 3D-Printed ULTEM 9085 Material *Addit. Manuf.* **13** 71–80

[9] Mohamed O A, Masood S H and Bhowmik J L 2017 Characterization and dynamic mechanical analysis of PC-ABS material processed by fused deposition modelling: An investigation through I-optimal response surface methodology *Meas. J. Int. Meas. Confed.* **107** 128–41

[10] Gardan N and Schneider A 2015 Topological optimization of internal patterns and support in additive manufacturing *J. Manuf. Syst.* **37** 417–25

[11] Langelaar M 2016 Topology optimization of 3D self-supporting structures for additive manufacturing *Addit. Manuf.* **12** 60–70

[12] Rezaie R, Badrossamay M, Ghaie A and Moosavi H 2013 Topology optimization for fused deposition modeling process *Procedia CIRP* **6** 521–6